

Optical Reddening, Integrated HI Optical Depth, Total Hydrogen Column Density

Harvey Liszt

*National Radio Astronomy Observatory
520 Edgemont Road, Charlottesville, VA 22903-2475*

hliszt@nrao.edu

ABSTRACT

Despite the vastly different angular scales on which they are measured, the integrated $\lambda 21$ cm HI optical depth measured interferometrically, Υ_{HI} , is a good proxy for the optical reddening derived from IR dust emission, with $\Upsilon_{\text{HI}} \propto E(\text{B-V})^{1.10}$ for $0.04 \text{ mag} \lesssim E(\text{B-V}) \lesssim 4 \text{ mag}$. For $E(\text{B-V}) \lesssim 0.04 \text{ mag}$ or $\Upsilon_{\text{HI}} < 0.7 \text{ km s}^{-1}$, less-absorbent warm and ionized gases assert themselves and $\tau(\text{HI})$ is a less reliable tracer of $E(\text{B-V})$. The $\Upsilon_{\text{HI}}\text{-}E(\text{B-V})$ relationship can be inverted to give a broken power-law relationship between the total hydrogen column density $N(\text{H})$ and Υ_{HI} such that knowledge of Υ_{HI} alone predicts $N(\text{H})$ with an accuracy of a factor 1.5 ($\pm 0.18 \text{ dex}$) across two orders of magnitude variation of Υ_{HI} . The $\Upsilon_{\text{HI}}\text{-}N(\text{H})$ relation is invariant under a linear rescaling of the reddening measure used in the analysis and does not depend on knowing properties of the HI such as the spin temperature.

Subject headings: astrochemistry . ISM: dust . ISM: HI. ISM: clouds. Galaxy

1. Introduction

The presence of a pervasive gaseous interstellar medium (ISM) was demonstrated over the course of several decades after Hartmann (1904) noted the presence of narrow, stationary absorption lines of NaI and CaII in the spectrum of the binary star δ Orionis. Ruling out the possibility that the lines were circumstellar took time and considerable ingenuity. Plaskett (1922) showed that the stationary lines observed toward HD47129 were at rest with respect to the Local Standard of Rest

(LSR), rather than the star. Struve (1928) noted the implied lumpy nature of the absorbing gas and showed that the integrated strength of the NaI D lines increased with stellar distance. Plaskett & Pearce (1930) showed that the Oort A-constant for the galactic rotation of the interstellar gas was just half that of the stars and it was generally accepted that the absorbing medium was distributed across the various sightlines and interstellar space.

The mean free path l or spatial frequency

($1/l$) of absorption features could be derived given the known stellar distances, and the discrete nature of the absorption lines gave rise to the notion of interstellar clouds of uncertain size but having a small volume filling factor¹ The discrete nature of the intervening matter was greatly reinforced by Münch’s analyses of the statistics of stellar color excesses and absorption line kinematics (Münch 1952, 1957), and the persistence of interstellar clouds led Spitzer (1956) to infer that they were bounded by an unseen but pervasive hot medium, the galactic corona. However, optical absorption lines proved to be problematic for understanding the ISM because of the difficulties in relating the strengths of lines from heavily depleted trace species in uncertain ionization states to hydrogen column densities (Eddington 1934, 1937; Routly & Spitzer 1952).

The discovery of $\lambda 21$ cm HI emission and the subsequent detection of HI absorption (Hagen et al. 1955; Clark et al. 1962; Clark 1965) and self-absorption (Heeschen 1955) provided gas kinetic temperatures (Field 1959) and hydrogen column densities of HI clouds as the optically-defined diffuse clouds came to be known to radio astronomers. In a smart synthesis, Spitzer (1968, 1978) put Münch’s color excesses on the modern scale of optical reddening $E(B-V)$ and related $E(B-V)$ to $\lambda 21$ cm HI hydrogen column density, directly translating Münch’s statistics to express the HI cloud column density distribution in terms of standard and large HI clouds having smaller and larger sizes, column densities and mean free paths.

Although a mean interstellar gas density

¹For uniform spheres the volume filling factor can be expressed as the ratio of diameter D to mean free path, $f_{\text{vol}} = 2/3 D/l$.

of approximately 1 H-atom cm^{-3} has been inferred since the early days of ISM studies (Oort 1932; Eddington 1934), Spitzer’s version of Münch’s mean color excess per unit distance, $\langle E(B-V)/l \rangle = 0.61 \text{ mag/kpc}$, is the modern origin of the widely-quoted mean ISM density, $1.2 \text{ H-nuclei cm}^{-3}$. The required conversion from reddening to hydrogen column density was for many years taken as $5.8 \times 10^{21} \text{ cm}^{-2} \text{ H-nuclei (mag)}^{-1}$ (Spitzer 1968, 1978; Bohlin et al. 1978; Savage et al. 1977) but we found $N(\text{H}) = 8.3 \times 10^{21} \text{ cm}^{-2} E(B-V)$ (Liszt 2014a,b) and other recent studies find ratios $7.7 - 9.4 \times 10^{21} \text{ cm}^{-2} \text{ H-nuclei (mag)}^{-1}$ (Hensley & Draine 2017; Lenz et al. 2017; Li et al. 2018). This is in part due to the suggested 14% downward scaling (Schlafly & Finkbeiner 2011) of the all-sky reddening maps of Schlegel et al. (1998).

In the course of our work defining the $E(B-V)$ - $N(\text{H})$ relation (Liszt 2014a,b), it was required to estimate the degree of saturation of HI emission profiles and this was accomplished by relating the integrated $\lambda 21$ cm HI optical depth $\Upsilon_{\text{HI}} \equiv \int \tau(\text{HI}) dv$ (units of km s^{-1}) to the all-sky map of FIR dust emission-derived reddening equivalent of Schlegel et al. (1998). Comparison of the separate relationships between the integrated HI emission and absorption with $E(B-V)$ defines a mean spin temperature- $E(B-V)$ relationship that directly indicates the degree of saturation in comparison with the observed HI brightness. We found that optical depth effects were not responsible for the larger $E(B-V)/N(\text{HI})$ ratios that are seen at $E(B-V) \gtrsim 0.07 \text{ mag}$ but see Fukui et al. (2015) for an opposing view.

Perhaps surprisingly given the vastly different angular scales on which they were measured, Υ_{HI} and $E(B-V)$ are tightly cou-

pled. From a combined sample of some 100 interferometric measurements of Υ_{HI} spanning 35 years we showed that there was a strong and very-nearly linear power-law relationship $\Upsilon_{\text{HI}} = 14.02 E(\text{B-V})^{1.07} \text{ km s}^{-1}$ for $0.02 \leq E(\text{B-V}) \lesssim 4$ mag: the lower limit on $E(\text{B-V})$ arises because weakly-absorbing warm or ionized hydrogen may dominate at $N(\text{H}) \lesssim 1 - 2 \times 10^{20} \text{ cm}^{-2}$ (Roy et al. 2013).

Recognizing that there are cases where the HI optical depth is measurable and the total hydrogen column density $N(\text{H})$ is not (for instance when CO observations are not available to estimate $N(\text{H}_2)$), the tight relationship between Υ_{HI} and $E(\text{B-V})$ suggests that Υ_{HI} can be a useful proxy for $N(\text{H})$ if that is simply related to $E(\text{B-V})$. Since our earlier discussion the SPONGE HI absorption sample has become available, adding some 50 new measurements of Υ_{HI} (Murray et al. 2018), and Roy et al. (2017) published a smaller sample of HI absorption measurements at especially low $E(\text{B-V})$. The larger ensemble of measurements of Υ_{HI} is employed in this work to better specify the $\Upsilon_{\text{HI}}\text{-}E(\text{B-V})$ relationship, to gain insight into the structure of the ISM, and to derive an empirical relationship that predicts $N(\text{H})$ from Υ_{HI} to an accuracy of ± 0.18 dex over a range of reddening and hydrogen column density spanning more than two orders of magnitude. The $\Upsilon_{\text{HI}}\text{-}N(\text{H})$ relation is invariant under a linear rescaling of the reddening measure used in the analysis. It can be used to infer other properties of HI in the ISM, but does not depend on knowing them.

The organization of this work is as follows. Section 2 is a discussion of Υ_{HI} , $E(\text{B-V})$ and the total column density of hydrogen nuclei $N(\text{H})$, where we derive relationships between Υ_{HI} and $E(\text{B-V})$ and Υ_{HI} and $N(\text{H})$

and discuss their implications for the constitution of the diffuse interstellar medium (ISM). Section 3 is a summary and discussion. In Appendix A we discuss an apparent disparity between integrated HI optical depths derived from interferometric and single-dish emission-absorption measurements.

2. Υ_{HI} and reddening

In this work, as before, we take $E(\text{B-V})$ from the FIR dust emission-derived equivalent optical reddening of Schlegel et al. (1998) (SFD), also occasionally denoted as $E(\text{B-V})_{\text{SFD}}$ when such a distinction is needed. As we discuss, the basic result of the present work, a relation between hydrogen column density and integrated $\lambda 21\text{cm}$ HI optical depth is independent of a linear rescaling of $E(\text{B-V})_{\text{SFD}}$.

Figure 1 shows the relationship between $E(\text{B-V})_{\text{SFD}}$ and various interferometrically-measured samples of the integrated HI optical depth Υ_{HI} . The left-most panel repeats the sample shown in Figure 3 of Liszt (2014b) using HI optical depths from Roy et al. (2013) and the sample assembled by Liszt et al. (2010), most of which is from the work of Dickey et al. (1983). The center panel shows more recent results from the new SPONGE survey (Murray et al. 2018) with data taken at the JVLA, and data from the sample of Roy et al. (2017) at low $E(\text{B-V})$ observed at the JVLA and GMRT. From the latter work we plot as 3σ upper limits all results with lower statistical significance. The SPONGE sample has more curvature but lies very nearly along the regression line defined by the larger sample of older measurements.

The solid line in each panel is the power-law regression fit to the data with $\Upsilon_{\text{HI}} \geq 0.07$

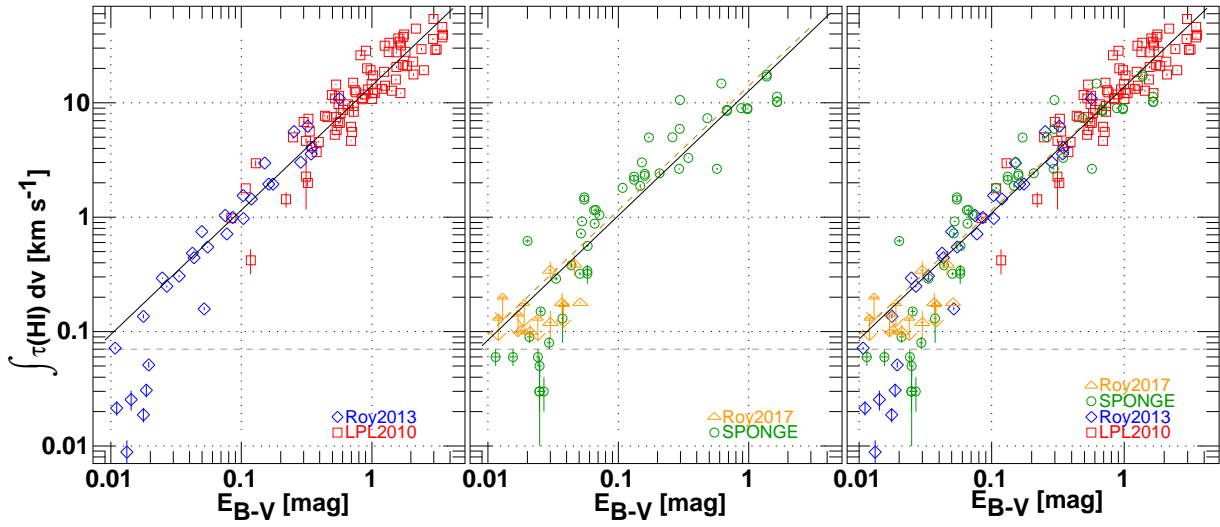


Fig. 1.— Integrated $\lambda 21$ cm HI optical depth for several samples, plotted against IR dust emission-derived optical reddening from Schlegel et al. (1998). Left: Interferometric HI optical depths from Roy et al. (2013) and the sample assembled by Liszt et al. (2010), most of which is from the survey of Dickey et al. (1983). Center: From the interferometric SPONGE survey (Murray et al. 2018) with data taken at the JVLA. Right: The merged sample from the two other panels. Solid lines are the power-law regression fits to the samples in each panel derived using data with $\Upsilon_{\text{HI}} \geq 0.07$ km s^{-1} and the dashed orange line in the center and right panels is the power-law fit derived from 107 sightlines in the panel at left. The regression fit for 160 sightlines with detections of HI absorption in the merged sample is $\Upsilon_{\text{HI}} = 13.80E(B-V)^{1.10}$ km s^{-1} .

km s⁻¹ and the dashed line in the center and right panels is the power-law fit derived from the 107 sightlines used in the regression fit at left. The combined sample of 160 sightlines at right has the regression line

$$\Upsilon_{\text{HI}} = (13.8 \pm 0.7) E(\text{B-V})^{(1.10 \pm 0.03)} \text{ km s}^{-1} \quad (1)$$

This has the very nearly the same slope and a 2% smaller multiplier than we determined previously (Liszt 2014b) from the sample shown at left using the data at $E(\text{B-V}) \geq 0.02$ mag.

As originally noted by Roy et al. (2013), Υ_{HI} is a less reliable indicator of $N(\text{HI})$ for $N(\text{HI}) \lesssim 2 \times 10^{20} \text{ cm}^{-2}$ (equivalently, $E(\text{B-V}) \lesssim 0.02 - 0.03$ mag) where the hydrogen is more likely to be warm or ionized and weakly-absorbing. This is also recognizable as the limiting column density defining the sample of damped Lyman-alpha (DLA) systems in the cosmological context of the Lyman-alpha forest, but galactic HI remains mostly neutral even at $E(\text{B-V}) = 0.01$ mag as shown in Figure 1 of Liszt (2014a). In any case, the full sample shows that the ability of Υ_{HI} to trace $E(\text{B-V})$ deteriorates at $E(\text{B-V}) \lesssim 0.04$ mag.

The demarcation of the warm \rightarrow cool HI transition seemed more clearly defined and at smaller $E(\text{B-V}) \lesssim 0.02$ mag in the older sample shown in the left-most panel of Figure 1. In the more recent data, hydrogen along sightlines with $E(\text{B-V})$ as large as 0.04 mag is not always dominated by cool, strongly-absorbing gas. Given that sightlines with $E(\text{B-V}) \gtrsim 0.07$ mag studied locally begin to show appreciable amounts of H_2 (Savage et al. 1977), there is only a narrow

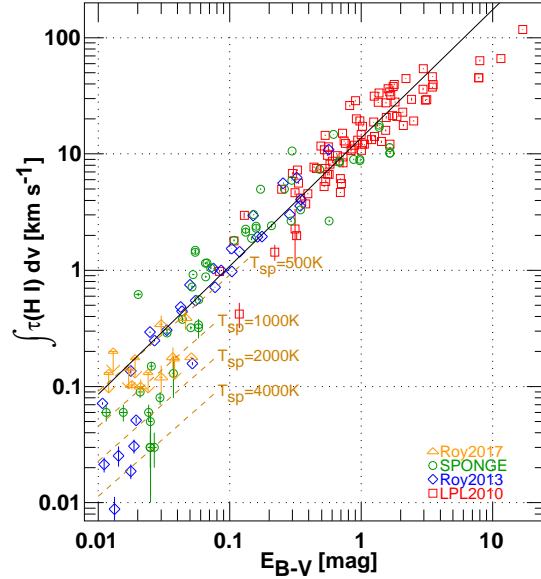


Fig. 2.— An extended view of the merged interferometric HI absorption sample. The regression line is the same as that shown in the rightmost panel of Figure 1, determined for $\int \tau(\text{HI}) dv \geq 0.07$ and $E(\text{B-V}) \leq 4$. Also plotted are curves of optical depth for $N(\text{HI}) = 8.3 \times 10^{21} \text{ cm}^{-2} E(\text{B-V})$ and HI spin temperature 500 K, 1000 K, 2000 K and 4000 K in a uniform, isothermal gas.

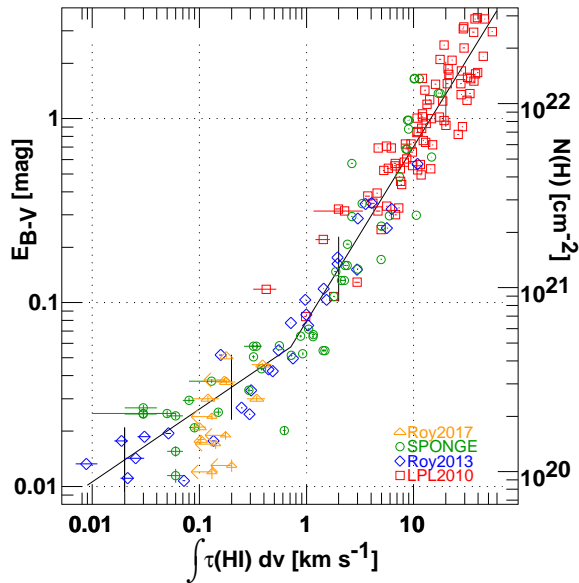


Fig. 3.— Reddening and implied $N(\text{H})$ vs Υ_{HI} . The data plotted at right in Figure 1 are shown with the variables interchanged and fit with two power laws meeting at $\Upsilon_{\text{HI}} = 0.72 \text{ km s}^{-1}$. Shown along the fitted curves are vertical markers denoting factor 1.5 (± 1.76 dex) variations. The scaling to $N(\text{H})$ uses $N(\text{H})/E(\text{B}-\text{V}) = 8.3 \times 10^{21} \text{ cm}^{-2} \text{ mag}^{-1}$ and is invariant to a linear re-scaling of $E(\text{B}-\text{V})$ as discussed in Section 2.3.

range of reddening over which the gas as a whole can be considered to be predominantly neutral, cool, and atomic. In this context it is also noteworthy how weak the integrated HI absorption is, as we now discuss.

2.1. Composition of the absorbing HI and its spin temperature

Shown in Figure 2 is an extended version of the rightmost panel of Figure 1, with the range in reddening extended to sightlines at very low galactic latitude and large reddening where $E(\text{B}-\text{V})_{\text{SFD}}$ is unreliable and the data do not follow the same power-law as for $E(\text{B}-\text{V})_{\text{SFD}} \lesssim 4 \text{ mag}$. The solid line in Figure 2 is the same regression line that is shown at right in Figure 1. Also superposed in Figure 2 are dashed lines of constant HI spin temperature T_{sp} that reproduce the plotted values of Υ_{HI} in a uniform atomic gas when $N(\text{HI}) = N(\text{H}) = 8.3 \times 10^{21} \text{ cm}^{-2} E(\text{B}-\text{V})$.

The spin temperatures that reproduce the integrated optical depths in a uniform gas are large compared to the emission line brightness, implying low optical depth. However, the spin temperatures that reproduce the regression line at $E(\text{B}-\text{V}) \lesssim 0.1 \text{ mag}$ are near 500 K and are unphysically large, given that specific determinations of the spin temperature in HI absorption profiles consistently put the typical kinetic temperatures of individual kinematic components below 100 K (Clark 1965; Dickey et al. 1978, 1979; Payne et al. 1982, 1983; Heiles & Troland 2003; Murray et al. 2018).

This disparity between the spin temperatures that reproduce the observed integrated HI optical depths and the kinetic temperatures of CNM imply that only a small fraction of the gas implied by the $E(\text{B}-\text{V}) - N(\text{H})$ conversion produces measurable HI absorption.

As an example, if the gas is artificially partitioned into an absorbing component with HI spin temperature 80 K and another that does not absorb at all, the proportion of absorbing gas at 80 K varies from 17% to 23% along the regression line. The SPONGE survey (Murray et al. 2018) concluded that 50% of the HI was detected in absorption. Overall, estimates of the molecular fraction of the diffuse ISM are in the range 25% - 40% (Bohlin et al. 1978; Liszt & Lucas 2002; Liszt et al. 2010), or roughly one-third. If one-third of the hydrogen in the diffuse ISM is in H₂ and 50% of the HI is detectable in HI absorption, the overall ionized gas fraction would be one-sixth.

2.2. Variation of E(B-V) with N(H)

A near-linear $\Upsilon_{\text{HI}}\text{-E(B-V)}$ proportionality could arise in a sufficiently well-mixed medium at large reddening, or if the gas observed at larger reddening were an accumulation of more parcels of the same gas that is seen at small reddening. However, the mix of strongly and weakly $\lambda 21\text{cm}$ -absorbing HI and unabsorbent ionized or molecular hydrogen is likely to vary over the wide range of reddening sampled in this work. Lines of sight with higher total E(B-V) are more likely to have a contribution from gas parcels that locally have relatively high E(B-V).

$\Upsilon_{\text{HI}}/\text{E(B-V)}$ increases with E(B-V) along the slightly-superlinear regression lines in Figures 1 and 2. Expressing

$$\Upsilon_{\text{HI}}/\text{E(B-V)} = \frac{\Upsilon_{\text{HI}}}{\text{N(H)}} \times \frac{\text{N(H)}}{\text{E(B-V)}} \quad (2)$$

one sees that gas with higher $\Upsilon_{\text{HI}}/\text{N(H)}$ and/or $\text{N(H)}/\text{E(B-V)}$ must increasingly be seen along the sightlines having higher total

E(B-V). However, Planck Collaboration et al. (2014) found that $\text{N(H)}/\tau_{353}$ decreased at higher column density, where τ_{353} is the 353 GHz dust optical depth that can be directly scaled to E(B-V) (see Appendix A). $\text{N(H)}/\text{E(B-V)}$ would presumably change in the same way and this acts in the wrong sense, depressing $\Upsilon_{\text{HI}}/\text{E(B-V)}$. To restore the observed behaviour $\Upsilon_{\text{HI}}/\text{N(H)}$ would have to increase by an even larger amount. This interplay between the properties of the dust and HI absorbing gas remain to be explored but the $\Upsilon_{\text{HI}}\text{-E(B-V)}$ relationship seems a general characteristic that should be explained by any model of the ISM.

2.3. Conversion from Υ_{HI} to N(H)

Figure 3 shows the data from the combined sample with the variables interchanged and N(H) calculated as $\text{N(H)}/\text{E(B-V)} = 8.3 \times 10^{21} \text{ cm}^{-2} \text{ mag}^{-1}$. The detections are well represented by two power laws, $\text{E(B-V)} = 0.0655\Upsilon_{\text{HI}}^{0.395} \text{ mag}$ for $\Upsilon_{\text{HI}} \leq 0.715 \text{ km s}^{-1}$ and $\text{E(B-V)} = 0.0788\Upsilon_{\text{HI}}^{0.950} \text{ mag}$ for $0.715 \text{ km s}^{-1} \leq \Upsilon_{\text{HI}} \leq 60 \text{ km s}^{-1}$. The break occurs at the same Υ_{HI} that was used as the lower-limit selection criterion to fit the E(B-V)- Υ_{HI} relationship of Eq. 1 as discussed in Section 2 and shown in Figure 1. The upper limits taken from the work of Roy et al. (2017) do not present constraints when the data are approximated in this way.

Shown along the power-law fits in Figure 3 are vertical bars indicating a span of ± 0.15 dex ($= 2^{1/2}$) and only a few points lie outside this range. The expected accuracy is therefore of this order. A Monte Carlo analysis with gaussian random errors in Υ_{HI} yields a 95% confidence limit of 0.18 dex, or a factor 1.5.

In terms of the column density

$$N(\text{H}) = A\Upsilon_{\text{HI}}^{0.395}, \Upsilon_{\text{HI}} \leq 0.715 \text{ km s}^{-1} \quad (3a)$$

and

$$N(\text{H}) = B\Upsilon_{\text{HI}}^{0.950}, 0.715 \text{ km s}^{-1} \leq \Upsilon_{\text{HI}} \quad (3b)$$

where $A = 5.43 \times 10^{20} \text{ cm}^{-2}$ and $B = 6.54 \times 10^{20} \text{ cm}^{-2}$.

It is important to note that the column density-integrated HI opacity relationship derived in this way uses the ratio $N(\text{H})/E(\text{B-V}) = 8.3 \times 10^{21} \text{ cm}^{-2} \text{ mag}^{-1}$ that we determined previously, but is independent of a linear rescaling of the $E(\text{B-V})_{\text{SFD}}$ values we used. The same result would have been derived now if we had earlier correlated $N(\text{HI})$ with $E(\text{B-V})'_{\text{SFD}} = 0.86 E(\text{B-V})_{\text{SFD}}$ suggested by Schlafly & Finkbeiner (2011), finding $N(\text{H})/E(\text{B-V}) = 9.65 \times 10^{21} \text{ cm}^{-2} \text{ mag}^{-1}$, and correlated Υ_{HI} with $E(\text{B-V})'_{\text{SFD}}$ now. Thus the ratio $N(\text{H})/E(\text{B-V}) = 8.3 \times 10^{21} \text{ cm}^{-2} \text{ mag}^{-1}$ is an important fiducial for the $N(\text{H})-\Upsilon_{\text{HI}}$ relationship, but the question of whether $E(\text{B-V})_{\text{SFD}}$ or $E(\text{B-V})'_{\text{SFD}}$ is the better measure of reddening is academic.

3. Summary and discussion

In Section 2 (see Figure 1) we discussed how the integrated $\lambda 21\text{cm}$ optical depth Υ_{HI} measured interferometrically is a good proxy for the reddening $E(\text{B-V})$ when $E(\text{B-V}) \gtrsim 0.04 \text{ mag}$ or $N(\text{H}) \gtrsim 2 - 3 \times 10^{20} \text{ cm}^{-2}$. Less absorbent ionized and warm neutral hydrogen make a noticeably larger proportional contribution to $N(\text{H})$ at $E(\text{B-V}) \lesssim 0.04 \text{ mag}$. From an updated HI absorption sample including sightlines from the recent SPONGE survey (Murray et al. 2018) and measurements from Roy et al. (2017) we derived the regression line $\Upsilon_{\text{HI}} = (13.8 \pm 0.7)E(\text{B-V})^{(1.10 \pm 0.03)} \text{ km s}^{-1}$.

As in our earlier work, the reddening measure we used was the IR dust-emission derived optical reddening equivalent of Schlegel et al. (1998) that we denoted as $E(\text{B-V})_{\text{SFD}}$ as necessary in the text.

Comparison of the observed integrated HI optical depths with the total hydrogen column densities implied by the ratio $N(\text{H})/E(\text{B-V}) = 8.3 \times 10^{21} \text{ cm}^{-2} \text{ mag}^{-1}$ from Liszt (2014a) in Section 2.1 showed that only a small fraction of the diffuse gas in the ISM is represented in HI absorption, as illustrated by the artificially high mean HI spin temperatures shown in Figure 2 for hypothetical gases comprised only of neutral atomic hydrogen. These high spin temperatures can be reconciled with measured kinetic temperatures below 100 K if only a fraction of the gas absorbs strongly in HI. Overall, the H-nuclei in the diffuse ISM are (approximately) one-third in H_2 and one-sixth in H^+ . One-half of the gas is in neutral hydrogen atoms and half of these are detected in absorption according to Murray et al. (2018). The fraction of the ISM gas overall that resides in the strongly-absorbing HI cold neutral medium (CNM) is about 20%.

In Section 2.2 we analyzed the slight super-linearity of the $\Upsilon_{\text{HI}} \propto E(\text{B-V})^{1.1}$ power-law relationship seen in Figure 1, expressing $\Upsilon_{\text{HI}}/E(\text{B-V}) = (\Upsilon_{\text{HI}}/N(\text{H})) \times (N(\text{H})/E(\text{B-V}))$ in Eq. 2 as the product of separate factors characterizing the HI-related and dust-related properties of the gas. At least one of those factors must increase with total $E(\text{B-V})$ to provide the observed 1.1 power-law slope. It is expected to find more high-column density parcels of colder HI at higher $E(\text{B-V})$, increasing $\Upsilon_{\text{HI}}/N(\text{H})$. However, (Planck Collaboration et al. 2014) found that $N(\text{H})/\tau_{353} \propto N(\text{H})/E(\text{B-V})$ decreased for

gas with higher $N(\text{H})$, implying the need for $\Upsilon_{\text{HI}}/N(\text{H})$ to increase even more rapidly with $E(\text{B-V})$. The larger issue is the extent to which $N(\text{H})/E(\text{B-V})$ varies and the extent to which such variations contribute to uncertainty in the generally-accepted single value that is in use.

In Section 2.3 (see Eqs. 3a and 3b) we assumed a value of $N(\text{H})/E(\text{B-V}) = 8.3 \times 10^{21} \text{ cm}^{-2} \text{ mag}^{-1}$ and inverted the $E(\text{B-V})$ - Υ_{HI} relationship to derive a broken power-law relation between Υ_{HI} and $N(\text{H})$ that reliably predicts the inferred $N(\text{H})$ from detections of Υ_{HI} to within a factor 1.5 (± 0.18 dex) for $0.01 \leq \Upsilon_{\text{HI}} \leq 60 \text{ km s}^{-1}$. As noted in Section 2.3 the $N(\text{H})$ - Υ_{HI} relationship so derived is independent of a rescaling of the reddening measure $E(\text{B-V})_{\text{SFD}}$ used to derive it, ie not affected by the 14% downward rescaling of the $E(\text{B-V})$ measure of Schlegel et al. (1998) that was suggested by Schlafly & Finkbeiner (2011). Nonetheless the $N(\text{H})/E(\text{B-V})$ ratio is an important quantity in its own right and it is not immune to uncertainty. Nguyen et al. (2018) recently derived $N(\text{H})/E(\text{B-V}) = 9.4 \times 10^{21} \text{ mag}^{-1}$ using 2MASS-derived reddenings, equivalent to a 13% downward rescaling of $E(\text{B-V})_{\text{SFD}}$. Lenz et al. (2017) derived $N(\text{H})/E(\text{B-V}) = 8.8 \times 10^{21} \text{ mag}^{-1}$ from a larger-scale comparison, but *after* a 12% downward rescaling, corresponding to the value $N(\text{H})/E(\text{B-V}) = 7.7 \times 10^{21} \text{ mag}^{-1}$ of Hensley & Draine (2017).

In Appendix A we showed that the most recent set of Arecibo singledish HI emission-absorption measurements (Heiles & Troland 2003), recently reviewed by Fukui et al. (2018), gave systematically larger Υ_{HI} than those measured interferometrically, especially at smaller Υ_{HI} and $E(\text{B-V})$. If this disparity

could be resolved, the sample of HI absorption measurements employed here might be substantially expanded.

The National Radio Astronomy Observatory is a facility of the National Science Foundation operated under contract by Associated Universities, Inc. I thank the Hotel Bel Éspérance in Geneva and the proprietor of Villa BEV in Mont-Jean (St. Barthelemy) for their hospitality during the completion of this manuscript. The manuscript was improved by the anonymous referee’s comments and suggestions for improvement.

A. Υ_{HI} from emission-absorption experiments

Heiles & Troland (2003) carried on a long tradition of simultaneous measurement of HI emission and absorption toward and around continuum sources at Arecibo (Dickey et al. 1978, 1979; Payne et al. 1982, 1983; Colgan et al. 1988). Their results, summarized and discussed recently by Fukui et al. (2018), are shown here in Figure 4. The Arecibo emission-absorption experiment finds a flatter Υ_{HI} -E(B-V) relationship and consistently larger Υ_{HI} than the interferometer sample at all E(B-V). The regression line fit to the Arecibo data at $\Upsilon_{\text{HI}} > 0.07 \text{ km s}^{-1}$ is $\Upsilon_{\text{HI}} = (17.0 \pm 1.6)E(\text{B-V})_{\text{SFD}}^{(0.975 \pm 0.049)} \text{ km s}^{-1}$, more nearly linear, but higher than that for the interferometrically-measured sample by factors of 2.19, 1.64 and 1.23 at $E(\text{B-V})_{\text{SFD}} = 0.01, 0.1$ and 1 mag, respectively. The origin of this difference remains to be investigated as it has not previously been recognized.

Fukui et al. (2018) tabulated values of the 353 GHz dust optical depth τ_{353} for the Arecibo emission-absorption sample in addition to Υ_{HI} so we generated $E(\text{B-V})_{\text{SFD}}$ and compared τ_{353} and $E(\text{B-V})_{\text{SFD}}$ as shown in Figure 5. With the exception of one widely-discrepant sightline at $E(\text{B-V})_{\text{SFD}} \approx 2$ mag, there is a tight linear relationship. The regression line fit is $\tau_{353}/10^{-6} = (68.2 \pm 2.7)E(\text{B-V})_{\text{SFD}}^{(1.020 \pm 0.018)}$ and this is only barely distinguishable from the τ_{353} -E(B-V)_{QSO} relationship of Planck Collaboration et al. (2014) using reddening values derived from photometry of SDSS QSO. That relationship, $\tau_{353}/10^{-6} = (67.1 \pm 1.3)E(\text{B-V})_{\text{QSO}}$ is also shown in Figure 5. The slope of a linear fit through the origin is $\langle \tau_{353} \rangle / \langle E(\text{B-V}) \rangle = 67.1 \times 10^{-6} \text{ mag}^{-1}$.

What is surprising in Figure 5 is not the linear relationship, but that the $\tau_{353}/E(\text{B-V})_{\text{SFD}}$ ratio is statistically indistinguishable from that predicted from the Planck τ_{353} -E(B-V)_{QSO} relationship of Planck Collaboration et al. (2014). $E(\text{B-V})_{\text{SFD}}$ is equivalent to $E(\text{B-V})_{\text{QSO}}$ for this eclectic collection of sightlines spanning quite a wide range of E(B-V) and a 14% downward scaling of $E(\text{B-V})_{\text{SFD}}$ is manifestly inappropriate for this sample.

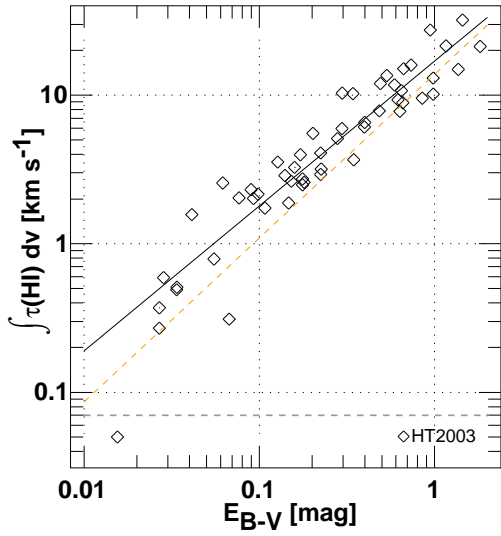


Fig. 4.— Integrated $\lambda 21$ cm HI optical depth from the Arecibo emission-absorption survey of Heiles & Troland (2003). The solid line is the regression line using all data with $\Upsilon_{\text{HI}} > 0.07$ mag as in Figure 1, $\Upsilon_{\text{HI}} = (17.0 \pm 1.6)E(\text{B-V})^{(0.975 \pm 0.048)} \text{ km s}^{-1}$. The dashed orange line is the power-law fit derived from the merged sample at right in Figure 1 with the same lower limit on Υ_{HI} .

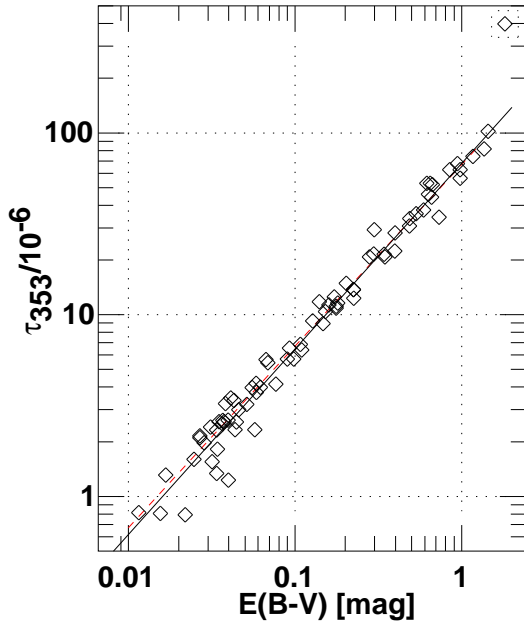


Fig. 5.— Planck 353 GHz dust optical depth τ_{353} vs. $E(B-V)$ from SFD98 for 76 lines of sight observed in $\lambda 21\text{cm}$ HI emission and absorption at Arecibo by Heiles & Troland (2003) (see Fukui et al. (2018) for the values of τ_{353} and Υ_{HI}). The regression relationship is $\tau_{353}/10^{-6} = (68.2 \pm 3.0)E(B-V)^{1.02 \pm 0.02}$ and the barely-visible red dashed line is the mean relationship between τ_{353} and reddening measured from quasar photometry by Planck Collaboration et al. (2014). The outlier point at the highest $E(B-V)$ was not used in the regression fit.

REFERENCES

- Bohlin, R. C., Savage, B. D., & Drake, J. F. 1978, *Astroph. J.*, 224, 132
- Clark, B. G. 1965, *Astroph. J.*, 142, 1398
- Clark, B. G., Radhakrishnan, V., & Wilson, R. W. 1962, *Astroph. J.*, 135, 151
- Colgan, S. W. J., Salpeter, E. E., & Terzian, Y. 1988, *Astroph. J.*, 328, 275
- Dickey, J. M., Kulkarni, S. R., Heiles, C. E., & Van Gorkom, J. H. 1983, *Astrophys. J., Suppl. Ser.*, 53, 591
- Dickey, J. M., Terzian, Y., & Salpeter, E. E. 1978, *Astrophys. J., Suppl. Ser.*, 36, 77
- . 1979, *Astroph. J.*, 228, 465
- Eddington, A. S. 1937, *The Observatory*, 60, 99
- Eddington, Sir, A. S. 1934, *Mon. Not. R. Astron. Soc.*, 95, 2
- Field, G. B. 1959, *Astroph. J.*, 129, 536
- Fukui, Y., Hayakawa, T., Inoue, T., Torii, K., Okamoto, R., Tachihara, K., Onishi, T., & Hayashi, K. 2018, *Astroph. J.*, 860, 33
- Fukui, Y., Torii, K., Onishi, T., Yamamoto, H., Okamoto, R., Hayakawa, T., Tachihara, K., & Sano, H. 2015, *Astroph. J.*, 798, 6
- Hagen, J. P., Lilley, A. E., & McClain, E. F. 1955, *Astroph. J.*, 122, 361
- Hartmann, J. 1904, *Astroph. J.*, 19
- Heeschen, D. S. 1955, *Astroph. J.*, 121, 569
- Heiles, C. & Troland, T. H. 2003, *Astroph. J.*, 586, 1067
- Hensley, B. S. & Draine, B. T. 2017, *Astroph. J.*, 836, 179
- Lenz, D., Hensley, B. S., & Doré, O. 2017, *Astroph. J.*, 846, 38
- Li, D., Tang, N., Nguyen, H., Dawson, J. R., Heiles, C., Xu, D., Pan, Z., Goldsmith, P. F., Gibson, S. J., Murray, C. E., Robishaw, T., McClure-Griffiths, N. M., Dickey, J., Pineda, J., Stanimirović, S., Bronfman, L., Troland, T., & PRIMO Collaboration. 2018, *Astrophys. J., Suppl. Ser.*, 235, 1
- Liszt, H. 2014a, *Astroph. J.*, 783, 17
- . 2014b, *Astroph. J.*, 780, 10
- Liszt, H. & Lucas, R. 2002, *A&A*, 391, 693
- Liszt, H. S., Pety, J., & Lucas, R. 2010, *A&A*, 518, A45+
- Münch, G. 1957, *Astroph. J.*, 125, 42
- Münch, I. G. 1952, *Astroph. J.*, 116, 575
- Murray, C. E., Stanimirovic, S., Goss, W. M., Heiles, C., Dickey, J. M., Babler, B., & Kim, C.-G. 2018, *ArXiv e-prints*
- Nguyen, H., Dawson, J. R., Miville-Deschênes, M.-A., Tang, N., Li, D., Heiles, C., Murray, C. E., Stanimirović, S., Gibson, S. J., McClure-Griffiths, N. M., Troland, T., Bronfman, L., & Finger, R. 2018, *Astroph. J.*, 862, 49
- Oort, J. H. 1932, *Bull. Astr. Inst. Neth.*, 6, 249
- Payne, H. E., Salpeter, E. E., & Terzian, Y. 1983, *Astroph. J.*, 272, 540

- Payne, H. E., Terzian, Y., & Salpeter, E. E. 1982, *Astrophys. J., Suppl. Ser.*, 48, 199
- Planck Collaboration, Abergel, A., Ade, P. A. R., Aghanim, N., Alves, M. I. R., Aniano, G., Armitage-Caplan, C., Arnaud, M., Ashdown, M., Atrio-Barandela, F., & et al. 2014, *A&A*, 571, A11
- Plaskett, J. S. 1922, *Mon. Not. R. Astron. Soc.*, 82, 447
- Plaskett, J. S. & Pearce, J. A. 1930, *Mon. Not. R. Astron. Soc.*, 90, 243
- Routly, P. M. & Spitzer, Jr., L. 1952, *Astroph. J.*, 115, 227
- Roy, N., Frank, S., Carilli, C. L., Mathur, S., Menten, K. M., & Wolfe, A. M. 2017, *Astroph. J.*, 834, 171
- Roy, N., Kanekar, N., Braun, R., & Chenguang, J. N. 2013, *Mon. Not. R. Astron. Soc.*
- Savage, B. D., Drake, J. F., Budich, W., & Bohlin, R. C. 1977, *Astroph. J.*, 216, 291
- Schlafly, E. F. & Finkbeiner, D. P. 2011, *Astroph. J.*, 737, 103
- Schlegel, D. J., Finkbeiner, D. P., & Davis, M. 1998, *Astroph. J.*, 500, 525
- Spitzer, L. 1968, *Diffuse matter in space* (New York: Interscience Publication, 1968)
- . 1978, *Physical processes in the interstellar medium* (New York Wiley-Interscience, 1978. 333 p.)
- Spitzer, Jr., L. 1956, *Astroph. J.*, 124, 20
- Struve, O. 1928, *Astroph. J.*, 67